MicroCT-based imaging of microvasculature within the bone tissue

David Haberthür[1,§], Oleksiy-Zakhar Khoma[1,§], Tim Hoessly[1], Eugenio Zoni[2,3], Marianna Kruithof-de Julio[2,3,4], Stewart D. Ryan[5], Myriam Grunewald[6], Benjamin Bellon[7], Rebecca Sandgren[8], Benjamin E. Pippenger[7,9], Dieter Bosshardt[9], Valentin Djonov[1], Ruslan Hlushchuk[1,*]

1: Institute of Anatomy, Universität Bern, Bern, Switzerland
2: Department for BioMedical Research, Urology Research Laboratory, University of Bern, Bern, Switzerland
3: Department of Urology, Inselspital, Bern University Hospital, Bern, Switzerland
4: Department for BioMedical Research, Translation Organoid Research, University of Bern, Bern, Switzerland
5: U-Vet Hospital, University of Melbourne Veterinary School, Werribee, Australia
6: Department of Developmental Biology and Cancer Research, Faculty of Medicine, The Hebrew University, Organoid Research Center, Hadassah University Hospital, Jerusalem, Israel
7: Preclinical and Translational Research, Institut Straumann AG, Basel, Switzerland
8: Centre for Comparative Medicine, Medical Faculty, Lund University, Lund, Sweden
9: Department of Periodontology, University of Bern, Bern, Switzerland
§: Equally contributing authors
*: Corresponding author: ruslan.hlushchuk@unibe.ch , +41 31 684 46 80

Abstract

Angiogenesis is a physiological process essential for skeletal development and growth, for bone healing and regeneration. Various research areas, including implantology and tissue engineering, would benefit from improved three-dimensional (3D) imaging of the vasculature within bone tissue.

In the last decades, X-ray microtomography (microCT) has gained recognition as a non-destructive 3D imaging technique for bone morphology. The structural nature of skeletal tissue has rendered the direct 3D imaging of its vasculature extremely difficult. For the detection of the vessels, contrast or casting agents must be used. A major drawback of such an approach has been the limited contrast between the common perfusion agents and mineralized tissue, which makes their distinct segmentation problematic. The usually applied decalcification resolves this issue but makes simultaneous assessment of the intracortical bone microstructure and the vascular morphology impossible. Moreover, the problem of contrasting becomes compounded in the presence of a metal implant.

Herewith we introduce the µAngiofil-enhanced microCT-based visualization of vasculature within bone tissue in various small and large animal models, with and without decalcification. This study documents simultaneous microvascular and bone imaging in murine tibia, murine bone metastatic model, pulp chamber, gingiva and periodontal ligaments. In a large animal model (minipig) we present the visualization and segmentation of different tissue types and vessels in the hemimandible containing several metal implants.

Herewith we provide for the first time a non-destructive 3D imaging approach of the vasculature within soft and hard tissues in the vicinity of metal implants in a large animal model.

Introduction

Angiogenesis is a physiological process essential for skeletal development and growth, for bone healing and regeneration; the established vascularization is crucial for successful bone formation and repair (Wernike et al., 2010, Roche et al., 2012, Carulli et al., 2013, Filipowska et al., 2017, Ren et al., 2022). Besides carrying nutrients and growth factors, the newly formed vessels are a delivery route of the stem cells and progenitors to the defect site (Kuttappan et al., 2018, Kurobane et al., 2019, Grosso et al., 2017). Moreover, age-related osteoporosis was shown to diminish with improved vascularization (Grunewald et al., 2021). There are many research areas which could benefit from an improved three-dimensional (3D) imaging of the vasculature within bone tissue: bone metastatic disease, bone biology, tissue engineering, implantology, reconstructive surgery and healing of both small and critical size bone defects with or without bone grafts. Most synthetic bone grafts fail to bridge critical sized defects due to their inability to promote vascularization (Lovett et al., 2009, Ren et al., 2022). Proper simultaneous non-destructive 3D imaging of the vasculature within bone tissue and of the bone tissue itself, especially in case of large bone grafts, has been a challenge for decades (Mercado-Pagan et al., 2015, Ren et al., 2022). The structural nature of skeletal tissue makes direct 3D imaging of its vasculature extremely difficult letting histology, a destructive and two-dimensional approach, remain a gold standard for years (Nunez et al., 2017). As blood vessels are encased in the calcified tissue, classic soft tissue imaging techniques such as light sheet microscopy or confocal laser scanning microscopy are challenging to apply (Nunez et al., 2017). Although, some promising advancements on tissue clearing-based imaging in case of craniofacial bones in mouse model have been recently published (Rindone et al., 2021, Luo et al., 2019).

In the last decades, X-ray micro-computed tomography (microCT) gained recognition as a non-destructive 3D imaging technique for bone morphology (Harrison and Cooper, 2015). For absorption-based X-ray microCT, the distinguishing vessels from other soft tissue structures within the bone structures is inhibited by the lack of noticeable differences in their respective X-ray absorption levels. It is thus necessary to use castings or instillation of contrast agents to unambiguously detect the vasculature. The available vascular replica-based imaging protocols improved the imaging of the vasculature within the bone, but had some serious drawbacks, such as disjoint vascular components and/or missing vascular segments (Schneider et al., 2009, Nunez et al., 2017). Another reported drawback issue was the limited contrast between the perfusion agent and mineralized tissue, which made their distinct segmentation problematic. To solve this issue, samples were usually decalcified prior to vascular imaging. The decalcification procedure makes simultaneous assessment of the intracortical bone microstructure and the vascular morphology impossible (Nunez et al., 2017).

Intravascular contrast-agent-enhanced microCT has the potential to overcome this obstacle. It has been applied and gained popularity as the method of choice for the evaluation of angiogenesis in bone tissue engineering and remodeling applications (Young et al., 2008, Roche et al., 2012, Ren et al., 2022). Barium sulfate and Microfil have been applied as the two most common contrast agents in studies about the vascularization of the bone tissue. Barium sulfate has been shown to provide a better perfusion and, correspondingly, visualization only in some selected studies (Roche et al., 2012). In many other studies, barium sulfate suspensions have been reported to have disadvantages such as higher viscosity, sometimes leading to incomplete vascular filling and weak or inhomogeneous signal

especially in higher resolution scans, due to particle aggregation (Krucker et al., 2006, Perrien et al., 2016, Leyssens et al., 2021). Although applied in probably a larger number of studies, Microfil was also reported to have many disadvantages, including poor and/or incomplete filling of the vasculature (Perrien et al., 2016, Hong et al., 2020, Roche et al., 2012, Leyssens et al., 2021).

The problem of contrasting becomes even further compounded in the presence of a metal implant. Such implants have revolutionized the treatment of patients with missing teeth or injured joints and bones (Yi et al., 2019, Raphel et al., 2016). The success of implant placement is believed to depend largely onto the interactions occurring near or at the implant-tissue interface (Yi et al., 2019, Bai et al., 2018). MicroCT is the only available approach to non-destructively investigate an intact bone-implant interface in 3D (Yi et al., 2019). Beyond the study of the anatomy and physiology of angiogenesis and vasculature of the bone organ, the contribution of the vascular component in the healing process around bone-borne implants is also considered an area of study meriting further experimentation (Ren et al., 2022, Al Subaie et al., 2015). To date, few studies have tried to visualize the vasculature surrounding implants using microCT imaging and, to the best of our knowledge, none have managed to resolve the micro-vascular component in a large animal model due to technical limitations of the perfused contrast agent and the applied microCT imaging technique.

With the present study we introduce the polymer-based contrast agent µAngiofil for microCT-based visualization of microvasculature within bone tissue in various small and large animal models, with and without decalcification of the bone. Moreover, we show that µAngiofil is suitable for simultaneous imaging and subsequent analysis of peri-implant hard and soft tissues as well as their vascularization in the vicinity of metal implants in a large animal model.

Method/Results

Animals

Animal procedures were performed in accordance with the applicable Swedish, Israeli or Swiss legislation on the protection of animals and were approved by the corresponding committees. In this study we used one transgenic VEGF male 21 months old mouse (see (Grunewald et al., 2021) for more details), five 6 weeks old CB17SCID male mice and two Göttingen minipigs.

Contrast-enhanced microangioCT of mice using µAngiofil

The contrast agent µAngiofil has been prepared according to the manufacturer's recommendations (Fumedica AG, Switzerland). The perfusion of the mice was performed as previously described (Hlushchuk et al., 2020, Hlushchuk et al., 2018). Briefly, heparinized animals were deeply anaesthetized, the thorax and the peritoneal cavity were opened with scissors to expose the descending aorta. The exposed aorta was then cannulated in either antegrade (for the perfusion of the hind limbs) or retrograde direction (for the perfusion of the head and teeth) with a Venflon cannula (26 GA). Afterwards, the blood was flushed out with warm PBS solution until the body part of interest turned completely pale. Three to four cuts of the liver edge allowed effusion of the blood and buffer solution. Thereafter, the corresponding (upper or lower) part of the body was perfused with µAngiofil at 1-1.5 ml/min using a syringe pump. The perfusion lasted until the organ of interest turned completely blue (Hlushchuk et al., 2019, Hlushchuk et al., 2018). In bones, it is not possible to visually monitor the described color change. Correct perfusion of the neighboring soft tissues serves as an indirect marker of the perfusion within the bone. Therefore, to achieve a good perfusion of the vessels within the bone, the perfusion time was significantly prolonged (at least 2 ml extra volume of contrast agent after all the superficial tissues of the extremity or head turned blue). Such a prolonged perfusion protocol ensured adequate perfusion of the bones of murine hind limbs (Fig. 1). After harvesting, the samples were fixed by immersion in 4% paraformaldehyde (PFA) solution and then scanned using microCT scanners (Bruker microCT, Kontich, Belgium). Figure 1 shows the bone microstructure and vascularization of a tibia of a 21-month-old VEGF transgenic male mouse. This visualization approach enabled a simultaneous display of bone, its vascularization, and their segmentation. Therefore, as presented in our other study, using the obtained datasets we could quantitatively show that the age-related osteoporosis diminishes with improved vascularization (Grunewald et al., 2021).

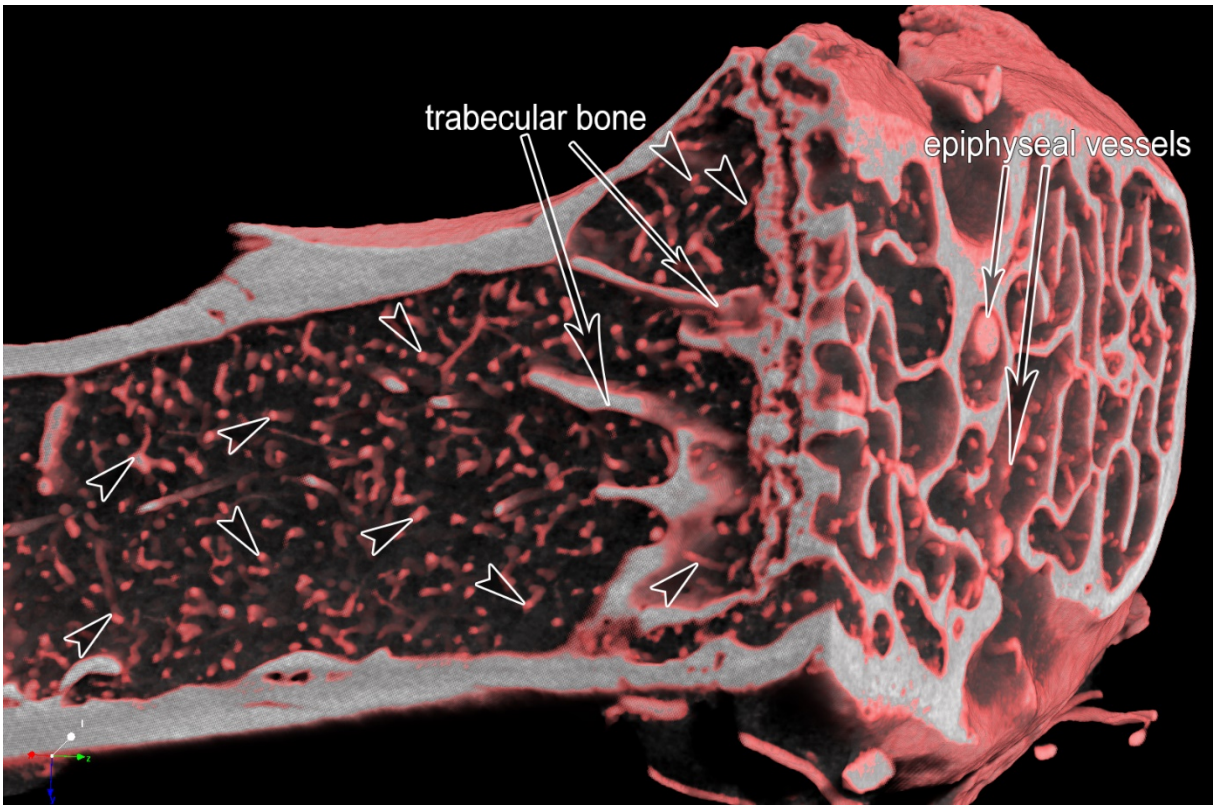

Fig. 1. MicroangioCT of proximal murine tibia of a 21-month-old VEGF transgenic male mouse. After perfusion with µAngiofil the murine tibia was harvested, fixated in 4% PFA and imaged by microCT. The arrowheads mark the visualized microvessels within the tibia. The diameter of the tibia shaft is around 1 mm. On the right side of the image one can distinguish the bigger epiphyseal vessels. The bone tissue appears white at the plane of the virtual section through the microCT-dataset. Scanning parameters (SKYSCAN 1172): acceleration voltage 50 kV, current 200 µA, 2.98 µm voxel size, 360 degrees scan, 0.05° rotation step, frame averaging 3.

Decalcification of the µAngiofil-perfused murine tibia

It is practically the standard in the field to decalcify the bone samples to enable the proper visualization and segmentation of vasculature within bone tissue (Nunez et al., 2017, Roche et al., 2012). Based on published data (Schneider et al., 2009), we were successful in establishing a bone-decalcifying protocol (for murine hind limb) with 10% EDTA solution (Schaad et al., 2017). Such a decalcification step does not seem to negatively influence the bone structure as such but reduces the X-ray absorption of bone tissue and renders it impossible to visualize it simultaneously with the vasculature (Fig. 2). On the other hand, it enables tomographic imaging of the murine hind limb vasculature with less artefacts around the bone at significantly lower acceleration voltage. In most instances it leads to remarkably shorter scanning times. Furthermore, segmentation of the vasculature in the tomographic datasets becomes easier and a subsequent histological evaluation of the sample is facilitated by such a decalcification step (Schaad et al., 2017).

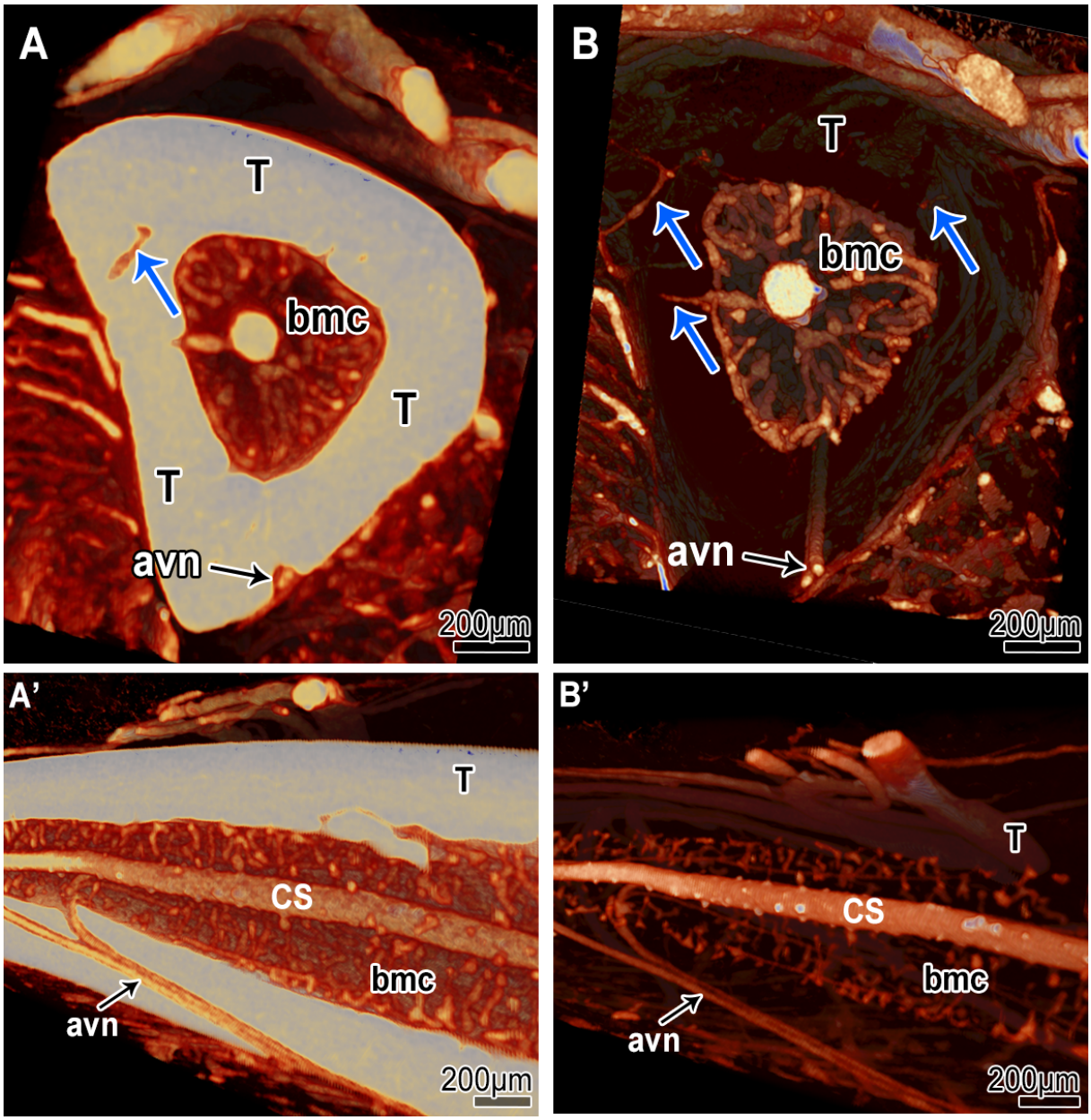

Fig 2. MicroangioCT-based visualization of the diaphysis of murine tibia before (A & A') and after decalcification with 10% EDTA (B & B'). Due to higher X-ray absorption the tibia bone appears brighter and non-transparent in A & A'. In B & B' it is transparent due to its lower X-ray absorption after decalcification. As a result, the connecting vessels between the periostal vessels and the vessels of the bone marrow cavity (bmc) are easily detectable (blue arrows in A & B). The visualization of the vessels within the medullar cavity (*central sinus* (CS)) is also improved. At the external surface of the tibia, supplying arteries are visible (*arteria et vena nutricia* (avn)). Scanning parameters (SKYSCAN 1172): acceleration voltage 59 kV, current 167 µA, 0.2 mm aluminum filter, 3.19 µm voxel size, 180 degrees scan, 0.1° rotation step, frame averaging 2.

Bone metastatic disease model, microangioCT

Assessment as well as 3D imaging of the tumor vasculature is always a challenging task, in almost every tumor model (Hlushchuk et al., 2016). A bone metastatic disease model is even more challenging for 3D microvascular imaging, due to the intraosseous location of tumor lesions. Since the changes in bone and vasculature are believed to be of crucial importance for

the progression of bone metastatic disease, simultaneous imaging of bone and vasculature is crucial. The desire to also simultaneously assess existing bone defects makes a decalcification procedure, as suggested above, extremely disadvantageous. To verify the suitability of our microangioCT approach for this kind of experimental imaging we used the following murine tumor model.

Murine bone metastatic disease model

In the bone metastatic disease model, 50000 PC3-M-Pro4Luc2 dTomato cells were injected into the tibia of 6 weeks old CB17SCID male mice as previously described (Zoni et al., 2019, Dai et al., 2016). The X-ray (25 kV, 6 sec) assessment (Faxitron Bioptics, Tucson, Arizona, US) was conducted at days 7, 14, 21 and 28 after implantation to monitor the progression of the lesions. Animal experiments were approved by the local ethical committee of the Canton of Bern, Switzerland (permit number BE 55/16) and carried out in accordance with Swiss Guidelines for the Care and Use of Laboratory Animals.

Prior to terminal anesthesia and perfusion with µAngiofil, the hind limb of interest was X-rayed using Faxitron Bioptics as a standard follow-up in this model (see insert in Fig. 3A). The harvested and fixated murine hind limb was then scanned using a desktop microCT scanner SKYSCAN 1272 (Fig. 3). The obtained dataset was reconstructed using NRecon Software v.1.7.4.2 (microCT Bruker, Kontich, Belgium) and visualized using CTvox Software v.3.3.1 (microCT Bruker, Kontich, Belgium). The visualization unambiguously displayed the intratumoral vasculature and extensive defects in the mineralized bone tissue. The neighboring structures, such as the growth plate, the epiphysis or the menisci are also easily assessed (Fig. 3).

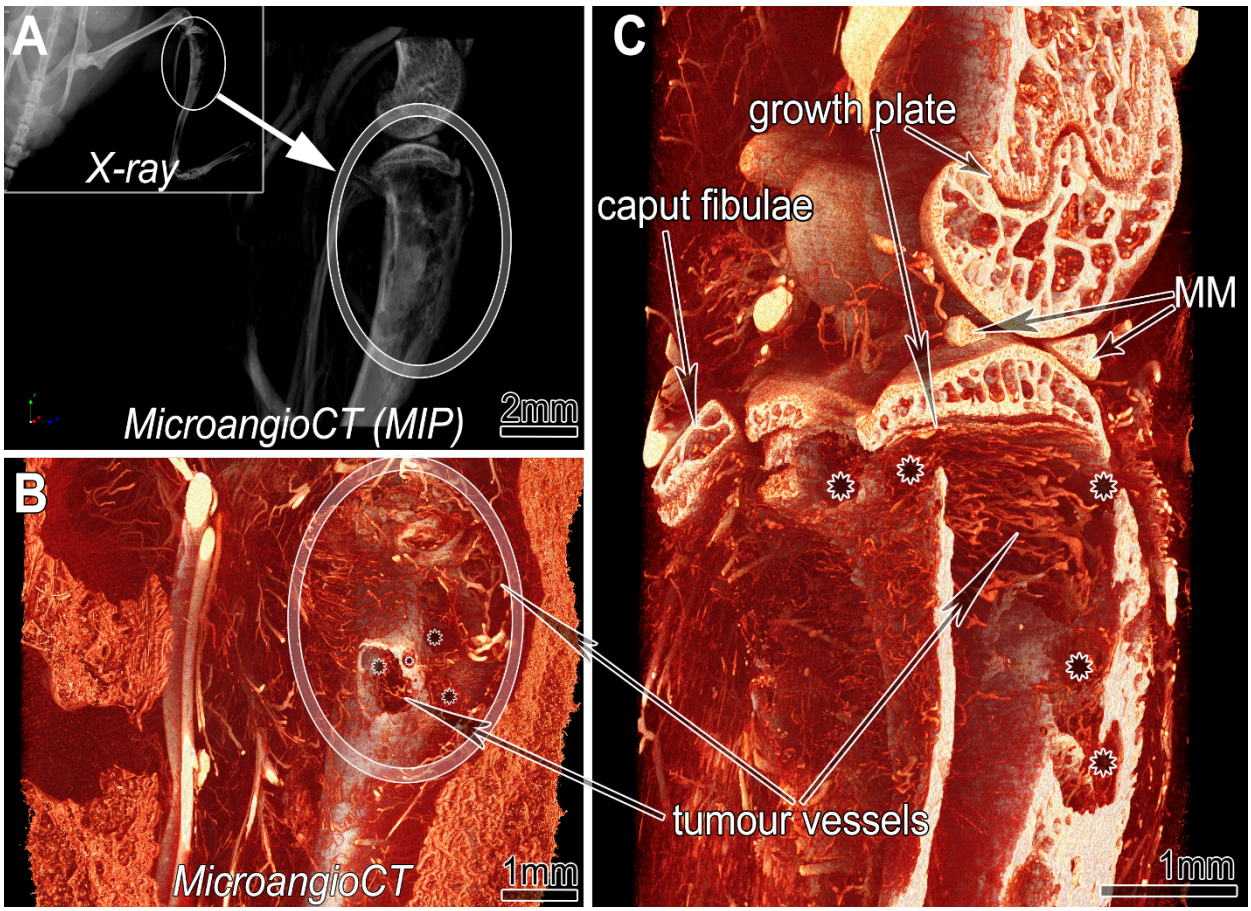

Fig. 3. MicroangioCT of a xenograft tumor implanted into the murine tibia. **A**: Maximum intensity projection (MIP) of the investigated hind limb segment indicated in the inserted X-ray image of the mouse prior harvesting. **B**: Virtual section through the obtained microangioCT dataset showing remarkable defects represented as holes (asterisks in B and C) in the tibial bone at the tumor site (encircled). **C**: A deeper positioned virtual section displaying the inner surface of the diseased tibia. Besides irregularly patterned tumor vessels (in B & C) further bony structures like growth plate or calcified parts of the medial meniscus (MM) are clearly distinguishable. Scanning parameters (SKYSCAN 1272): acceleration voltage 60 kV, current 166 µA, 0.2 mm aluminum filter, 1.65 µm voxel size, 360 degrees scan, 0.1° rotation step, frame averaging 3.

MicroangioCT of murine mandible/teeth

Murine mandibles and teeth are challenging samples due to the location of most of the vessels within the bone canals or in the proximity of the hard tissue and, correspondingly, the lack of larger bone-free volumes in which the vessels are easily distinguishable. Nonetheless, with the improved perfusion protocol (see above) and a well visualized difference between the X-ray absorption levels of µAngiofil and mineralized bone tissue, we achieved appropriate imaging of the sample. The microvasculature of murine mandible, periodontal ligament, and the teeth (even within their pulp chamber) can be clearly visualized without undergoing a decalcification procedure (Fig. 4).

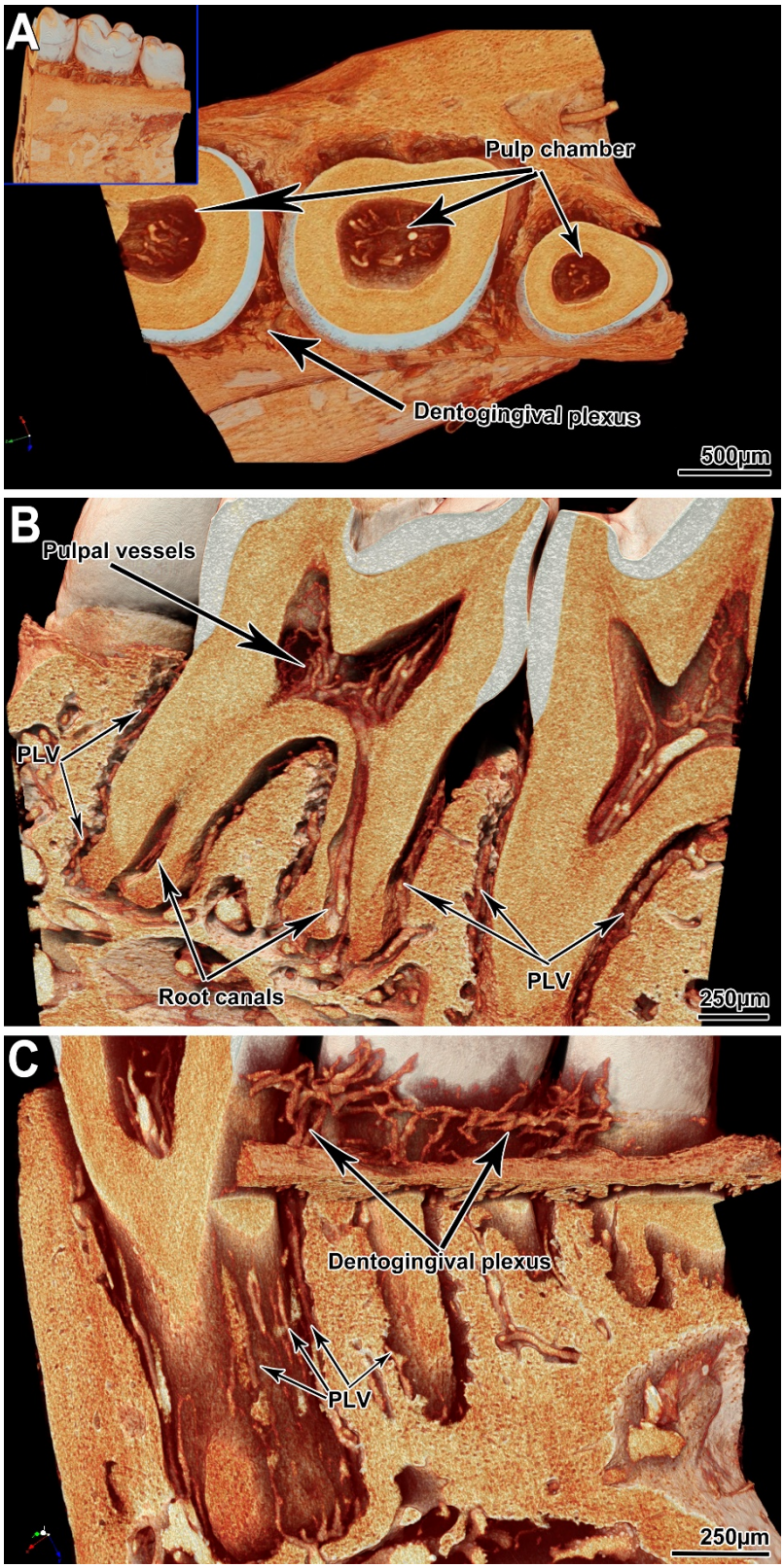

Fig. 4. MicroangioCT of the vasculature of murine teeth. A: View onto the virtual horizontal section through the crowns of the murine teeth: The pulp chambers are visible, and the pulpal vessels are presented. Overview of the dataset in the inset at the upper left corner. **B**: Sagittal section through the mandible. The microvessels within the pulp cavities and root canals are distinct. **C**: A closer view onto the dentogingival plexus and periodontal ligament vessels (PLV). Scanning parameters (SKYSCAN 1172): accelerating voltage 80 kV, voxel size 1.0 µm, 0.2 mm aluminum filter, rotation step 0.1°, 360 degrees scan, frame averaging 4.

MicroangioCT of mandible in a large animal model (Göttingen Minipig)

Due to their similarity to humans in terms of anatomy, bone structure and bone remodeling, the Göttingen Minipig has become a well-accepted large animal model in preclinical dental and orofacial research (Wang et al., 2007, Pearce et al., 2007, Herring et al., 2011). The stricter legal requirements regarding primates and the societal resistance against the use of companion animals, such as dogs and cats, have further enhanced the usage of Göttingen minipigs as animal models (Pearce et al., 2007).

Göttingen minipigs (Ellegaard Göttingen Minipig, Dalmose, Denmark) held under license 5.8.18-15672/2019 approved by the Malmö/Lund regional ethical committee, Sweden, were intramuscularly anesthetized (25-35 mg/kg, Dexdomitor; Orion Pharma Animal Health and 50-70 mg/kg, Zoletil 100 Vet, Virbac) and heparinized with 300 IE/kg intravenously (Heparin LEO, LEO Pharma). After heparin infusion, the pigs were euthanized with an intravenous dose (100 mg/kg) of pentobarbital (Euthanimal vet, VM Pharma). *A. carotis externa* was accessed by blunt dissection through tissue of the ventral neck and cannulated (BD Venflon, 17G). After washing out the blood with PBS, the corresponding head side was selectively perfused with µAngiofil through the arterial tree. The success of the perfusion has been visually controlled equivalent to the previously described perfusion in mice. After polymerization of µAngiofil (~30 min), the mandible was excised and fixated in 4% PFA solution. They were later scanned using SKYSCAN 2214 or SKYSCAN 1273, and the datasets reconstructed and visualized using NRecon v.1.7.4.2 and CTvox Software v.3.3.1, correspondingly (both microCT Bruker, Kontich, Belgium). Our approach provides excellent imaging of the whole mandible vasculature down to the vessels within the root canals and pulp chamber (Fig. 5).

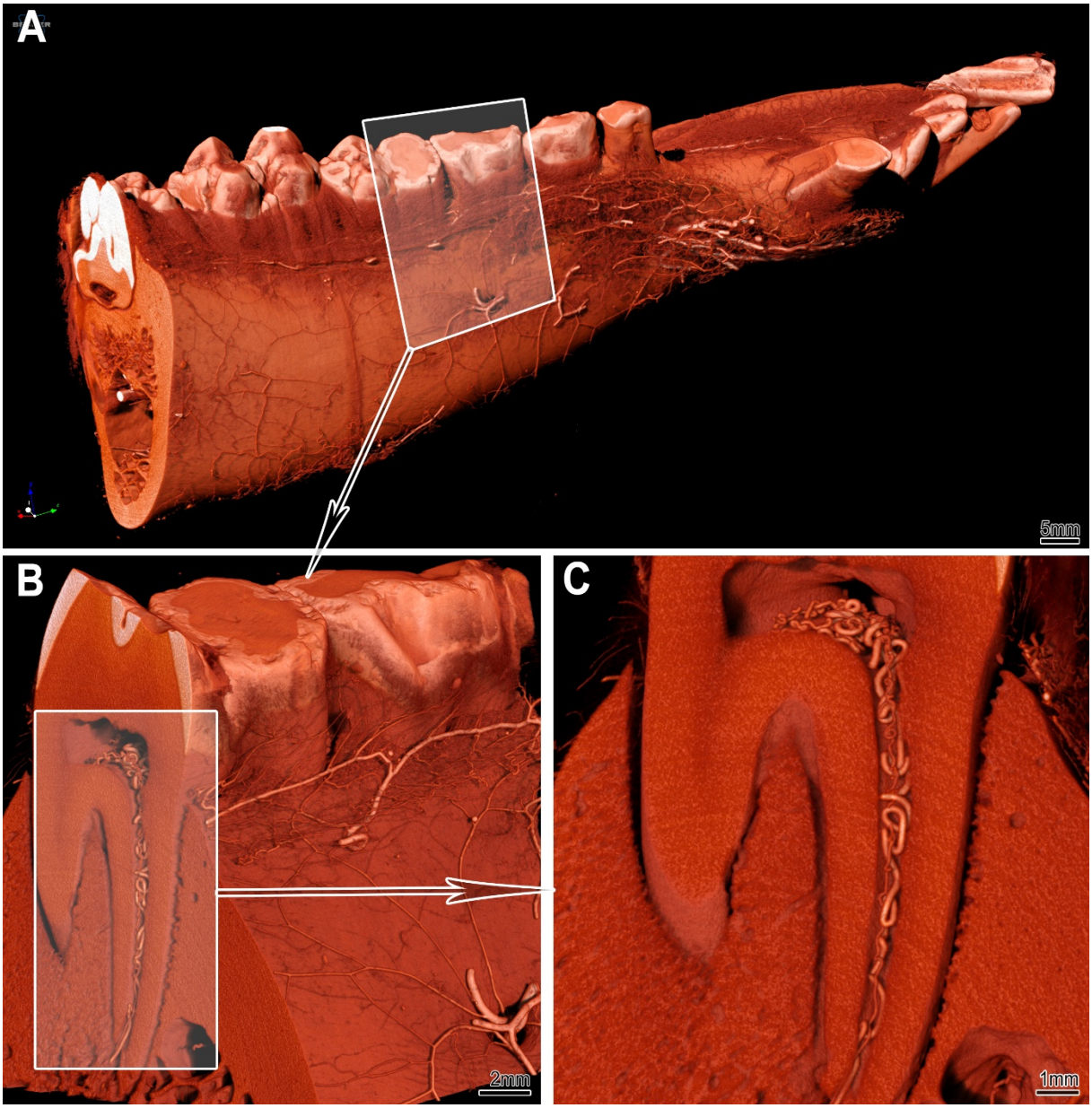

Fig 5. MicroangioCT of the minipig mandibula. Panel A displays the visualization of a right minipig hemimandible: the vasculature at the bone surface is clearly visible. The framed area in A marks the subvolume represented in panel B at higher magnification. Panel C displays the transverse section marked in panel B: the pulp chamber and root canal with the corresponding vessels are unambiguously visualized. Scanning parameters for images in panel A (SKYSCAN 1273) accelerating voltage 100 kV, current 80 µA, 9 µm voxel size, 1 mm aluminum and 0.2 mm copper filter, rotation step 0.15°, 360 degrees scan, frame averaging of 5. Scanning parameters for images in panels B and C (SKYSCAN 2214): accelerating voltage 100 kV, current 100 µA, 8 µm voxel size, 1 mm copper filter, 0.18° rotation step, 360 degrees scan, frame averaging 4. Due to the voxel size of 8-9 µm, the microvessels with diameter of approx. 40 µm or less cannot be visualized in such large samples.

As already mentioned, the Göttingen Minipig has become a very popular large animal model in dental research and is often used also for implantology studies. After researchers in the field realized that osseointegration is influenced by angiogenesis, there is understanding that

angiogenesis and, correspondingly, vascular supply of the peri-implant tissue should be assessed as thoroughly as possible and preferably in 3D. So far, the only reliable approach to assess the vascular supply remains histology, which is limited to single two-dimensional sections. Based on the findings in those single histological sections, researchers try to assess the vascularization of the peri-implant bone. Even for the microCT approach, it is a challenging task due to the presence of metal parts and, therefore, multiple objects with high density within the samples. The decalcification step could reduce the density of the sample but would inevitably lead to the loss of information on the bone microstructure making the simultaneous assessment of the bone and vessels impossible (Nunez et al., 2017). Another obstacle is to have a contrast agent that can be distinctly separated from both the metal implants and the mineralized tissue. With µAngiofil it is easily possible to visualize and distinguish between soft tissue, bone tissue, contrast agent-filled vessels as well as metal implants according to their gray values in the histogram (Fig. 6). Such imaging does not require bone decalcification and enables a rather straightforward segmentation of features of interest without cumbersome post-processing (Fig. 6D).

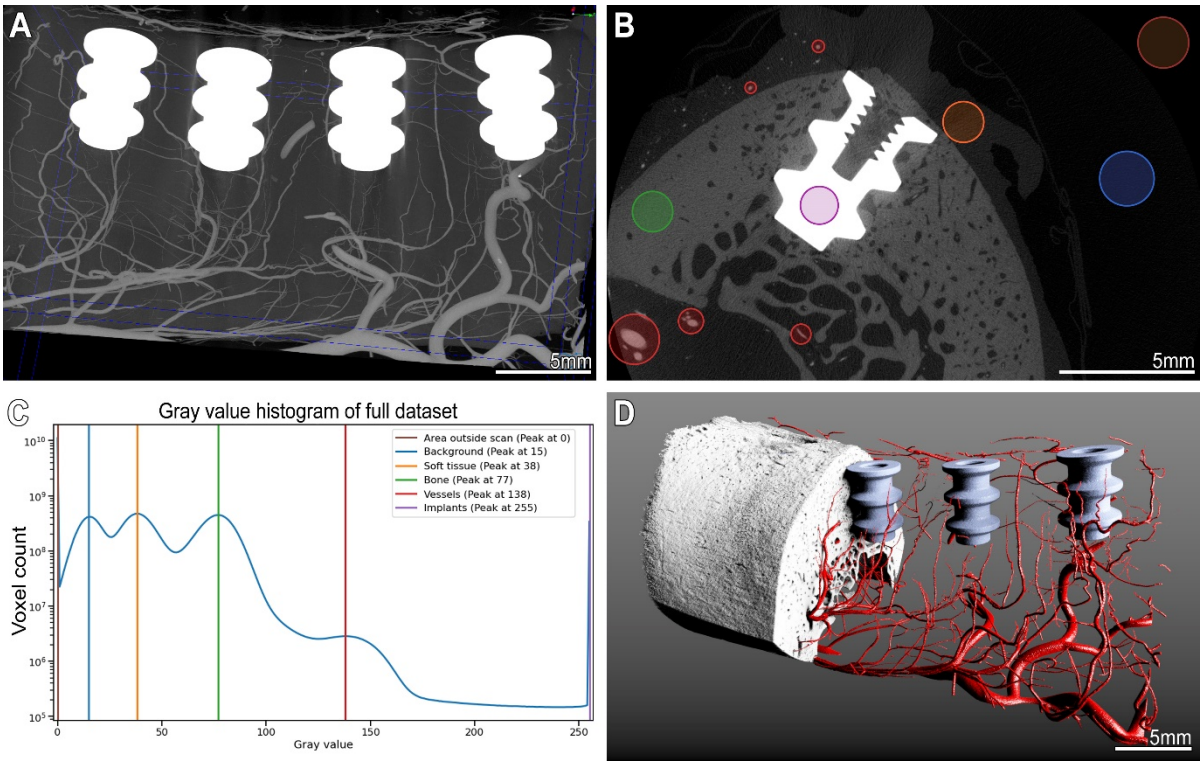

Fig 6. MicroangioCT of the peri-implant vasculature of a minipig mandibula. Panel A displays a MIP image of the minipig mandible with 4 metal implants and µAngiofil–perfused vessels. Panel B: virtual transversal section through an implant within the mandible. Structures with distinguishably different grey values are marked with colored circles – see the histogram distribution and corresponding peaks with colors legend in panel C. Such differences in grey levels allow a straightforward segmentation of the structures of interest as displayed in panel D. Scanning parameters (SKYSCAN 2214): accelerating voltage 100 kV, voxel size 8.0 µm, 1 mm copper filter, rotation step 0.18°, 360 degrees scan, frame averaging 4.

Discussion

There is an understanding in the bone biology, tissue engineering and related research fields, that adequate vascularization is a prerequisite for successful bone formation and regeneration as well as osseointegration of biomaterials (Li et al., 2022, Schott et al., 2021, Sivaraj and Adams, 2016, Wernike et al., 2010, Chandra and Atala, 2019). To influence or even control these processes, the interplay between vascular and bone tissue should be studied at the most detailed imaging level available.

During the last decades, microCT gained recognition as a non-destructive 3D imaging technique for bone morphology (Harrison and Cooper, 2015), and is considered the only available approach for 3D imaging of an intact bone-implant interface (Yi et al., 2019). Unfortunately, the microCT-based distinction of the vessels from other soft tissue structures is not possible without intravascular casting or instillation of contrast agents. Moreover, although enabling the visualization of the vasculature, most such casting or contrast agents are difficult to distinguish from the non-demineralized bone tissue due to the lack of remarkable differences in their X-ray absorption levels (Young et al., 2008). For example, in case with Microfil, the mentioned lack of contrast requires decalcification of the samples before the bone vasculature can be properly visualized with a microCT scanner (Nunez et al., 2017, Young et al., 2008). Some studies have described that barium sulfate suspension could be used for direct simultaneous imaging of vasculature and bone (Schneider et al., 2009, Qiu et al., 2016). Many studies report higher viscosity of this agent in comparison to Microfil or µAngiofil, though which leads to inconsistent vascular filling or even the inability to perfuse fine capillaries (Leyssens et al., 2021, Qiu et al., 2016). The hereby described approach with µAngiofil provides more complete vascular filling (Hlushchuk et al., 2020, Leyssens et al., 2021) and is suitable for the visualization of the microvasculature within bone tissue with or without decalcification (Fig. 2). If a subsequent histological evaluation is desired, the developed decalcifying protocols enable correlative imaging of the same sample with preserved intravascular contrast agent (Schaad et al., 2017).

Distinct differences in the attenuation between the µAngiofil and bone tissue allow for assessing vascularization and bone growth without the need to make two scans (before and after decalcification) and register them, saving labor, scanning time and without damaging the sample composition.

The presented here microangioCT approach can be used for simultaneous visualization of the hard (and eventually soft) tissues and their vascularization in a variety of small and large animal models. One of the noteworthy possible applications of this approach is simultaneous visualization of the bone microarchitecture and microvasculature of the bone metastases in the murine xenograft tumor model (Fig. 3). Using such an approach, the response to specific treatments, including bone-targeted and antiangiogenic therapies, can be assessed within the same sample and in 3D, followed by histological examination if needed (Xu et al., 2022). The gained results could provide further insights onto yet not completely elucidated interplay between angiogenesis and bone growth, bone lysis and bone turnover. The results will be crucial for selecting potential drug candidates and proper treatment decision and efficacy prediction. The decalcification step would be very disadvantageous for bone metastatic models, since pathological processes in the bone tissue should be thoroughly assessed because they may lead to so-called skeletal-related-events, which are associated with shortened survival and deterioration of quality of life (D'Oronzo et al., 2019), and should therefore be avoided.

In dental research, preclinical models can be divided into small and large animals. Besides more practical size, small animal models (e.g., mouse) are very popular in the research labs, including dental ones, and less expensive. Moreover, there is a variety of genetically modified lines available which could facilitate imaging if using corresponding imaging modalities (Yi et al., 2019). The microCT scan of correspondingly small samples perfused with µAngiofil can be performed with a voxel size around 1 µm, leading to an excellent detail resolution (Fig. 4).

Nonetheless, the small size of hemimandible samples and availability of the transgenic lines allow another recently published imaging approach in the murine models. This recently described PEGASOS tissue-clearing-based approach could be a viable option for the visualization of the peri-implant tissues and vasculature in small animal models (Yi et al., 2019). Among the most significant limitations of this tissue-clearing-based imaging approach are: i) differential shrinkage among soft and hard tissues, leading to anisotropic distortion in samples where both tissue types (plus eventual metal implant) are present; ii) limited depth (e.g., around 800 µm in a mouse model) due to the challenges of achieving complete transparency of bone tissue (Yi et al., 2019). These limitations become even more critical in a big animal model with metal implants. Large anisotropic distortion of the sample may lead to the alteration of the common site of interest, namely the implant-tissue interface. Furthermore, the actual limitation of the depth makes such an approach completely impracticable.

The microangioCT approach does not have such limitations and can be easily applied for visualization of hemimandible and its vascularization in a large animal model like Göttingen minipig (Fig.5). µAngiofil has noticeably different attenuation than mineralized bone and it is useful when scanning the samples, which contain high-density materials, like metals. It is thus possible to visualize and distinguish soft tissue, bone tissue, vessels filled with the contrast agent as well as metal implants according to their gray values in the histogram (Fig. 6).

To the best of our knowledge, this is the first study demonstrating non-destructive three-dimensional imaging of the microvasculature of bone in the proximity of metal objects/implants in a large animal model.

Limitations of the approach

The most significant limitation of the suggested approach is the general limitation of microCT imaging, namely, the correlation between the resolution and the sample size. If the sample is small, i.e. only a few millimeters in diameter, the voxel size may be as small as 1 µm or less enabling visualization of the microvasculature down to the capillary bed (Hlushchuk et al., 2019, Hlushchuk et al., 2020, Hlushchuk et al., 2018, Schaad et al., 2017). In case of large samples, like minipig hemimandible, the achievable voxel size is around 10 times larger (≥8 µm), and it is therefore, not possible to reach that level of resolution. In such samples the finest microvessels with diameter under 40 µm cannot be accurately visualized (see Fig. 5 & 6).

Nonetheless, the presented approach is, according to our knowledge, the best what can be achieved with the modern microCT scanners and is a big step forward for qualitative and quantitative imaging in tissue engineering and implantology research as well as many other related research fields.

References

Al Subaie AE, Eimar H, Abdallah MN, et al. (2015) Anti-VEGFs hinder bone healing and implant osseointegration in rat tibiae. *J Clin Periodontol,* **42,** 688-96.

Bai L, Liu Y, Du Z, et al. (2018) Differential effect of hydroxyapatite nano-particle versus nano-rod decorated titanium micro-surface on osseointegration. *Acta Biomater,* **76,** 344-358.

Carulli C, Innocenti M, Brandi ML (2013) Bone vascularization in normal and disease conditions. *Front Endocrinol (Lausanne),* **4,** 106.

Chandra P, Atala A (2019) Engineering blood vessels and vascularized tissues: technology trends and potential clinical applications. *Clin Sci (Lond),* **133,** 1115-1135.

D'Oronzo S, Coleman R, Brown J, Silvestris F (2019) Metastatic bone disease: Pathogenesis and therapeutic options: Up-date on bone metastasis management. *J Bone Oncol,* **15,** 004-4.

Dai J, Hensel J, Wang N, Kruithof-de Julio M, Shiozawa Y (2016) Mouse models for studying prostate cancer bone metastasis. *Bonekey Rep,* **5,** 777.

Filipowska J, Tomaszewski KA, Niedzwiedzki L, Walocha JA, Niedzwiedzki T (2017) The role of vasculature in bone development, regeneration and proper systemic functioning. *Angiogenesis,* **20,** 291-302.

Grosso A, Burger MG, Lunger A, Schaefer DJ, Banfi A, Di Maggio N (2017) It Takes Two to Tango: Coupling of Angiogenesis and Osteogenesis for Bone Regeneration. *Front Bioeng Biotechnol,* **5,** 68.

Grunewald M, Kumar S, Sharife H, et al. (2021) Counteracting age-related VEGF signaling insufficiency promotes healthy aging and extends life span. *Science,* **373**.

Harrison KD, Cooper DM (2015) Modalities for Visualization of Cortical Bone Remodeling: The Past, Present, and Future. *Front Endocrinol (Lausanne),* **6,** 122.

Herring S, Li Y, Liu Y, et al. (2011) Oral Biology and Dental Models.), pp. 491-516.

Hlushchuk R, Barre S, Djonov V (2016) Morphological Aspects of Tumor Angiogenesis. *Methods Mol Biol,* **1464,** 13-24.

Hlushchuk R, Haberthur D, Djonov V (2019) Ex vivo microangioCT: Advances in microvascular imaging. *Vascul Pharmacol,* **112,** 2-7.

Hlushchuk R, Haberthur D, Soukup P, et al. (2020) Innovative high-resolution microCT imaging of animal brain vasculature. *Brain Struct Funct,* **225,** 2885-2895.

Hlushchuk R, Zubler C, Barre S, et al. (2018) Cutting-edge microangio-CT: new dimensions in vascular imaging and kidney morphometry. *Am J Physiol Renal Physiol,* **314,** F493-F499.

Hong SH, Herman AM, Stephenson JM, et al. (2020) Development of barium-based low viscosity contrast agents for micro CT vascular casting: Application to 3D visualization of the adult mouse cerebrovasculature. *J Neurosci Res,* **98,** 312-324.

Krucker T, Lang A, Meyer EP (2006) New polyurethane-based material for vascular corrosion casting with improved physical and imaging characteristics. *Microsc Res Tech,* **69,** 138-47.

Kurobane T, Shiwaku Y, Anada T, et al. (2019) Angiogenesis involvement by octacalcium phosphate-gelatin composite-driven bone regeneration in rat calvaria critical-sized defect. *Acta Biomater,* **88,** 514-526.

Kuttappan S, Mathew D, Jo JI, et al. (2018) Dual release of growth factor from nanocomposite fibrous scaffold promotes vascularisation and bone regeneration in rat critical sized calvarial defect. *Acta Biomater,* **78,** 36-47.

Leyssens L, Pestiaux C, Kerckhofs G (2021) A Review of Ex Vivo X-ray Microfocus Computed Tomography-Based Characterization of the Cardiovascular System. *Int J Mol Sci,* **22**.

Li Y, Fraser D, Mereness J, et al. (2022) Tissue Engineered Neurovascularization Strategies for Craniofacial Tissue Regeneration. *ACS Appl Bio Mater,* **5,** 20-39.

Lovett M, Lee K, Edwards A, Kaplan DL (2009) Vascularization strategies for tissue engineering. *Tissue Eng Part B Rev,* **15,** 353-70.
Luo W, Yi Y, Jing D, et al. (2019) Investigation of Postnatal Craniofacial Bone Development with Tissue Clearing-Based Three-Dimensional Imaging. *Stem Cells Dev,* **28,** 1310-1321.
Mercado-Pagan AE, Stahl AM, Shanjani Y, Yang Y (2015) Vascularization in bone tissue engineering constructs. *Ann Biomed Eng,* **43,** 718-29.
Nunez JA, Goring A, Hesse E, Thurner PJ, Schneider P, Clarkin CE (2017) Simultaneous visualisation of calcified bone microstructure and intracortical vasculature using synchrotron X-ray phase contrast-enhanced tomography. *Sci Rep,* **7,** 13289.
Pearce AI, Richards RG, Milz S, Schneider E, Pearce SG (2007) Animal models for implant biomaterial research in bone: a review. *Eur Cell Mater,* **13,** 1-10.
Perrien DS, Saleh MA, Takahashi K, et al. (2016) Novel methods for microCT-based analyses of vasculature in the renal cortex reveal a loss of perfusable arterioles and glomeruli in eNOS-/- mice. *BMC Nephrol,* **17,** 24.
Qiu X, Shi X, Ouyang J, Xu D, Zhao D (2016) A method to quantify and visualize femoral head intraosseous arteries by micro-CT. *J Anat,* **229,** 326-33.
Raphel J, Holodniy M, Goodman SB, Heilshorn SC (2016) Multifunctional coatings to simultaneously promote osseointegration and prevent infection of orthopaedic implants. *Biomaterials,* **84,** 301-314.
Ren Y, Senarathna J, Grayson WL, Pathak AP (2022) State-of-the-art techniques for imaging the vascular microenvironment in craniofacial bone tissue engineering applications. *Am J Physiol Cell Physiol,* **323,** C1524-C1538.
Rindone AN, Liu X, Farhat S, et al. (2021) Quantitative 3D imaging of the cranial microvascular environment at single-cell resolution. *Nat Commun,* **12,** 6219.
Roche B, David V, Vanden-Bossche A, et al. (2012) Structure and quantification of microvascularisation within mouse long bones: what and how should we measure? *Bone,* **50,** 390-9.
Schaad L, Hlushchuk R, Barre S, et al. (2017) Correlative Imaging of the Murine Hind Limb Vasculature and Muscle Tissue by MicroCT and Light Microscopy. *Sci Rep,* **7,** 41842.
Schneider P, Krucker T, Meyer E, et al. (2009) Simultaneous 3D visualization and quantification of murine bone and bone vasculature using micro-computed tomography and vascular replica. *Microsc Res Tech,* **72,** 690-701.
Schott NG, Friend NE, Stegemann JP (2021) Coupling Osteogenesis and Vasculogenesis in Engineered Orthopedic Tissues. *Tissue Eng Part B Rev,* **27,** 199-214.
Sivaraj KK, Adams RH (2016) Blood vessel formation and function in bone. *Development,* **143,** 2706-15.
Wang S, Liu Y, Fang D, Shi S (2007) The miniature pig: a useful large animal model for dental and orofacial research. *Oral Dis,* **13,** 530-7.
Wernike E, Hofstetter W, Liu Y, et al. (2010) Long-term cell-mediated protein release from calcium phosphate ceramics. *J Biomed Mater Res A,* **92,** 463-74.
Xu H, Lafage-Proust MH, Bouazza L, et al. (2022) Impact of Anti-Angiogenic Treatment on Bone Vascularization in a Murine Model of Breast Cancer Bone Metastasis Using Synchrotron Radiation Micro-CT. *Cancers (Basel),* **14**.
Yi Y, Men Y, Jing D, et al. (2019) 3-dimensional visualization of implant-tissue interface with the polyethylene glycol associated solvent system tissue clearing method. *Cell Prolif,* **52,** e12578.
Young S, Kretlow JD, Nguyen C, et al. (2008) Microcomputed tomography characterization of neovascularization in bone tissue engineering applications. *Tissue Eng Part B Rev,* **14,** 295-306.
Zoni E, Astrologo L, Ng CKY, et al. (2019) Therapeutic Targeting of CD146/MCAM Reduces Bone Metastasis in Prostate Cancer. *Mol Cancer Res,* **17,** 1049-1062.